

*Research article*

## **Mathematical modelling of the Eddy current and its application to the material examinations**

*Murat Vural*

*Mechanical Engineering Department, Faculty of Mechanical Engineering, Istanbul Technical University  
Istanbul, Turkey*

*Received 01 August 2012*

*Revised 31 October 2012*

*Accepted 08 November 2012*

### **Abstract**

Eddy Current testing, especially the Preventive Multi-Frequency Testing (PMFT) method is being used on C45R steel material, under the control of specialities like microstructure and stiffness characteristics. The physical principles of eddy current is examined theoretically, and the applications of the procedure are shown experimentally. Eddy currents can easily be used in determination of heat treatment differences of forging steel. As heat treatment conditions change, microstructure and stiffness differences that can occur especially on surface and locations near the surface of components cause some changes in permeability particularly, in high test frequencies. Eddy current can outshine by causing big changes in bobbin impedance.

©2012 Usak University all rights reserved.

**Keywords:** *Eddy current, preventive multi-frequency testing (PMFT), inductive reactance, impedance plane*

### **1. Introduction**

Increasing quality needs has also enhanced the importance of the Eddy Current testing procedure, which is one of the non-destructive material examination procedures. This procedure is a reliable and quite economic test method [1,2]. The Eddy Current testing, especially the Preventive Multi-Frequency Testing (PMFT) method has a wide application area [3]. It is used under the control of specialities like microstructure and stiffness characteristics of every types of materials successfully all around the world. In this work, firstly the physical principles of eddy current is examined theoretically, and then the applications of the procedure are shown experimentally [1,2].

### **2. The Method**

#### **2.1. Description of the method**

The Eddy current method basically depends on the electromagnetism, the basic of conductors' examination. There is a magnetic area around a conducting electric current. The power of this magnetic area is directly proportional with the current that forms the area. This variable current creates a pulsating magnetic area. An

electricconducting material is placed into this magnetic area; a voltage will be inducted inside this material. Since the material is a conductor, this voltage induces a current inside the material. This current is known as “Eddy Current”. The Eddy current has the same characteristics with its constituent current but in the opposite direction. The Eddy current on the surface of material is directly related to its constituent current’s frequency. Thus, the depth where the Eddy current affects will decrease as this frequency grows. The Eddy current that occurred inside the material surface is related to phase changes of the currents occurred on the surface. If the Eddy currents encounter material failures such as fracture, cavities, surface damage or defective source integrations, they cannot spread through expected direction. This results in a change in the magnetic area, and the test bobbin also reacts due to this change. The Eddy currents are used in determination of this conception material failure through a test procedure [2-5].

Eddy currents are inducted in test material; however, they do not uniformly distribute inside the entire material. Eddy currents are quite dense on surface, and they decrease as entering into material exponentially [6]. The distance that the Eddy currents can enter into material effectively is called the depth of penetration. Standard depth of penetration is calculated with the formula given in (1).

$$\delta = \sqrt{\frac{1}{\pi \cdot f \cdot \mu_0 \cdot \mu_r \cdot \sigma}} \quad (1)$$

where;  $\delta$ : Standard depth of penetration (m),  $\sigma$ : Conductivity of the material,  $f$ : frequency (hertz),  $\mu_r$ : relative permeability and  $\mu_0$ : permeability of the space.

Standard depth of penetration is equal to 1/e of the eddy current on the surface. This is also known as the depth of the skin. Practically, the Eddy current density decreases to 0.7% value of that on the surface.

## 2.2. Basic Principles of the Procedure

If alternate current is passed through a transmitter bobbin, a magnetic area will occur inside the bobbin [7]. If the test sample is approached to the current-transporter bobbin, the Eddy currents will be inducted on this test sample. This is schematically shown in Fig.1. The amplitude of the Eddy currents depends on the chemical composition and the structural conditions (i.e, stiffness) of the material. By changing the frequency of the currents, the electromagnetic “fingerprint” of the structural situation inside the bobbin system can be obtained. The differences emerged from the structural situation, the compound, the material involvement; the wrong heat treatment applications will cause changes in the Eddy current signals. Test devices recognize these types of changes and show the deviations. Advanced test systems function by using Preventive Multi-Frequency Testing (PMFT) method. This speciality also allows detection of unforeseen failures in wide frequency band intervals [7].

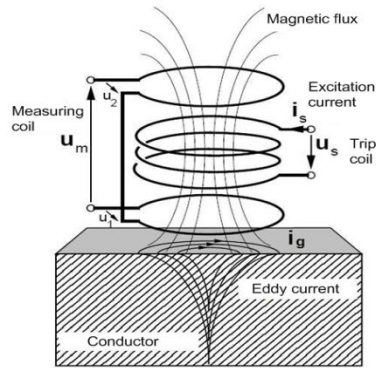


Fig. 1 Occurrence and detection of the eddy currents [2]

### 2.3. Ability of the Procedure

The procedure of the Eddy currents can be applied to any material that is an electrical or a magnetic conductor. This includes all metallic materials. It must be known that the structural test procedure through Eddy current is a comparison attitude rather than an exact measurement method. For instance, Eddy current test device used in application can clearly discriminate hardness differences of 2-3 HRC. However, the scan ends with yes or no. The Eddy current test device will recognize measured changes in the test component with respect to current tolerance interval; however, it will not interest their causes. To get exact answers, hardness test of findings of device or its affirmation through the metallographic tests can be made [2,5,8].

### 2.4. Mathematical Modelling

When alternating current (AC) is applied to an Eddy current system, the current passes through inductive reactance ( $X_L$ ) and the resistance ( $R$ ). In Fig.2, inductive reactance voltage is shown as  $E_1$  and resistance voltage is shown as  $E_2$ . The specific voltage value is equal to the product of current and inductive reactance or resistance.

$$E_1 = I \cdot X_L \text{ and } E_2 = I \cdot R \quad (2)$$

Inductive reactance voltage  $E_1$  has a phase difference of  $90^\circ$  from  $E_2$ . These two voltages are shown in Fig.2. At any moment, in the voltage plane diagram, since the value of the current that passes through the inductive reactance and resistance is equal, the voltage values' ratio over the current value can give the inductive reactance and resistance values. The diagram obtained is named as phase vector or phaser diagram and reveals the amplitude and phase relations at the same frequency (Fig.2).

When inductive reactance and resistance values are variable, voltage decrease in the system varies with these values and the decrease of voltage. Impedance is shown by different impedance phaser,  $Z$ , in the plane(1-2). The total decrease of voltage equals to vectoral sum of  $E_r$ ,  $E_1$  and  $E_2$ .

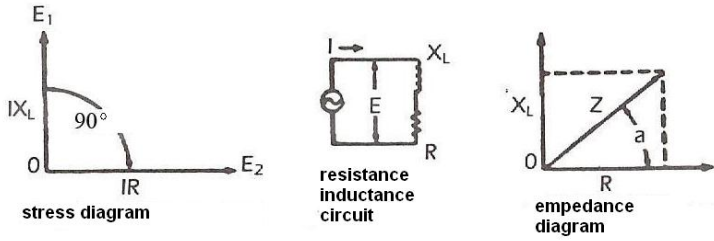


Fig. 2 Voltage and impedance plane diagrams [3]

$$Z = X_L + R \text{ or } Z = \sqrt{X_L^2 + R^2} \quad (3)$$

These voltage values are related with the resistance, reactance and frequency of the system. Decrease of voltage through the resistance is directly proportional with IR, the product of resistance and current. Decrease of voltage through the reactance is proportional with both inductance (L) and frequency (f) (1.3).

$$X_L = 2 \cdot \pi \cdot f \cdot L \quad (4)$$

Vectoral sum of reactance and resistance making 90° with each other gives the impedance value Z and the angle of lag. Generally, the test bobbins are characterized with two impedance values;

- Inductive reactance  $X_L$  (alternate current frequency hertz; self inductance of bobbin, L, henry unit)
- Ohmic resistance (R).

Generally, in the impedance plane, reactance ( $X_L$ ) is drawn as vertical axes and resistance (R) is drawn as horizontal axes. In this way, the impedance of test bobbin, Z, is expressed with a P point that is formed as perpendicular to two components in impedance plane. When test component is not inside the bobbin, the characteristic impedance of the bobbin  $P_0$  that has  $X_{L0}$  and  $R_0$  coordinates, shown as "bobbin-air" in impedance plane in the Fig. 3. If the bobbin is placed upon the test component, the original area of the bobbin in the air is newly changed with the Eddy currents. Even if the characteristic of test bobbin changes, that obtained change stays the same. The effect of test component is expressed as the change in the characteristics of test bobbins. The impedance of the bobbin in the air,  $P_0$  has changed to the  $P_1$  (with new  $X_L$  and R values) due to the effect of test component (Fig.3).

The direction and amplitude of impedance from  $P_0$  to  $P_1$  depend on the characteristics of test component and the device. The important characteristics of the test components are:

- Electrical conductivity ( $\sigma$ )
- Size of the test component
- Magnetic permeability ( $\mu$ )
- Discontinuities like fracture

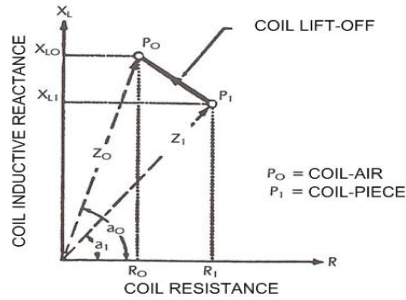


**Fig. 3** Illustration of the characteristic of test bobbin in impedance plane [3]

### 2.5. Conductivity and Permeability Curves on Impedance Plane

Responds of conductivities that belonged to various non-magnetic compounds on impedance plane is given in Fig.4. With increase of conductivity through clockwise material characteristic draws an orbit similar to comma. Bobbin lift-off curves for different materials are also shown. As seen, for titanium, the angle between conductivity and lift-off curves is smaller than those for copper. Thus, unexpected lift-off variable occurred while testing copper or aluminium compounds at 100 kHz, and this will have less effect on test than those for titanium or graphite. The space between conductivity curves shows a characteristic that is not linear. For instance, on the upper point of the curve, the space between titanium and 304 stainless steel is larger than that between bronze and aluminium on the bottom point.

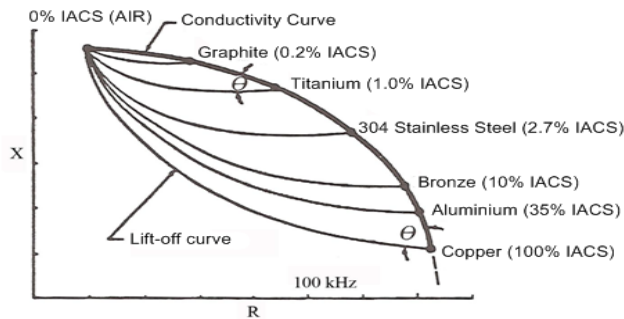


**Fig. 4** Conductivity and lift-off curves on impedance plane [3]

For non-magnetic compounds, the effects of test frequency over the conductivity and lift-off curves are shown in Fig. 5. As seen in Fig. 5, the frequency changes cause a non-linear dislocation on the conductivity curve. This case is also valid for other impedance curves and can be used as an advantage. In high frequencies (Fig. 5c), the separation angle between lift-off and conductivity curves of the bronze is quite small. Thus, removing the lift-off is very difficult. In lower frequencies (Fig. 5a), the separation angle  $\theta$  of bronze is larger. And that allows the removal of lift-off and perception of conductivity changes with high sensitivity. 500 kHz and 1 Mhz interval must be selected for separation of titanium compounds. Test frequency selected for separation of aluminium compounds must be in 20 kHz and 100 kHz interval. Generally, for conductivity test (compound separation, control of heat treatment etc.) and control of surface fractures, frequency must be selected just below the convolution of conductivity curve of the material.

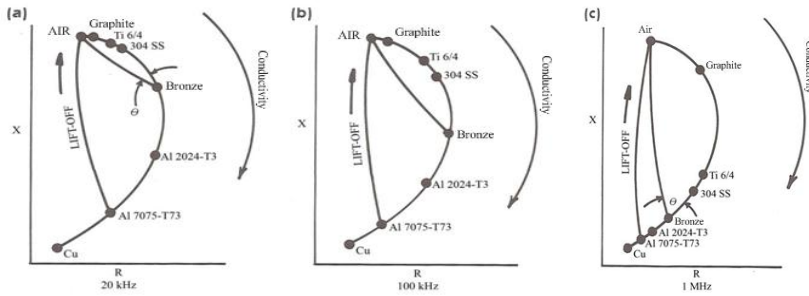


**Fig. 5** Change of frequency: (a) Lowfrequency (b) Medium frequency (c) High frequency [4]

For magnetic materials, lift-off and magnetic permeability curves are almost in an added position to each other (Fig. 6a). Despite of this, values of each of them increases throughreverse directions. If a magnetic material, for instance, ferrous is placed inside the magnetic area of the bobbin, the opposite situation can be observed. Because the magnetic force of the current bobbin puts atomic magnetic elements inside the material in order coherently to magnetic area; thus, the flux density increases. This effect is defined with the following Eq. 5.

$$B = \mu \cdot H \tag{5}$$

where; B: Magnetic flux density,  $\mu$  : Magnetic relative permeability and H: Magnitude of magnetic force or magnetic area.

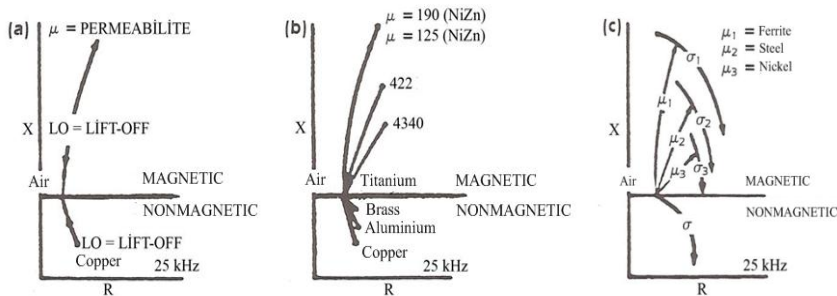


**Fig. 6** Permeability, lift-off and conductivity curves on impedance plane: (a) Permeability and lift-off curves. (b) Permeability curves for different materials. (c) Permeability and conductivity curves [3]

As an example, with low conductivity and two different permeability values, NiZn ferrite nuve is choosen. The increase of flux density results in a big increase in the test bobbin voltage. And this causes an increase in the impedance. The increase in the impedance is in the direction of the reactance except small energy losses due to the effects of hysteresis. Since inductive reactance is a function of inductance and frequency, for different frequencies, the phase angle of impedance vector varies. Thus, three points of the vector move along the curve as frequency changes. Change in the phase angle of 4340 quality steel for 75-300 kHz was shown in Fig. 7.

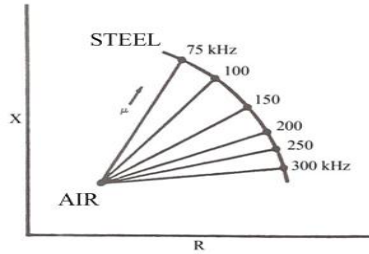


Fig. 7 Change in angle of phase on the impedance plane due to change of frequency [4]

### 3. Experimental Studies

Today's concept of quality control is based on 100% control of the products, considering all products should be controlled by various means. Especially after heat treatment, material properties can be kept under control with the eddy current method.

In the experimental works, automobile front parts provided from steel forging manufacturer firm were used as the test samples (Fig. 8). Current test samples were also produced from the same material. During our work, various heat treatment processes were applied to these materials.



Fig. 8 General view of the test samples

In this part, C45R steel is being used as the test material, and the chemical analysis result is given in Table 1. C45R steel has a chemical composition that is convenient for solidifying in terms of carbon content, and at the end of the reform process, it shows high toughness against definite draught levels.

Table1

The chemical composition of the steel C45R used in the experiments

Wt%	C	Si	Mn	P	Ni	S	Mo	Cr
Standart	0.42-0.5	Max 0.4	0.5-0.8	Max 0.4	Max 0.03	0.02 -0.4	Max 0.4	Max 0.1
Experimental	0.478	0.27	0.76	0.009	0.028	0.15	0.01	0.06

Tempering can be defined by first applying hardening then age-tempering processes to achieve high toughness for the steel workpiece. The general heat treatment characteristics of the material C45R are given in Table 2.

**Table2**

The heat treatment specialities of the steel C45R [4]

Normalisation temperature	Heating temperature for hardening	Quenching ambient	Tempering temperature
840 – 880°C	820 – 860°C	Water or Oil	550 – 660°C

In the experimental study, a device and some test bobbins were used. This device is convenient for multi-frequency test technique, simultaneously works in 8 different frequencies. It is a sensitive Eddy current test device. Eight selected frequencies are applied relatively, and impedance differences in receiver bobbin windings were measured. The total test duration was in milliseconds. Some absolute bobbins are used in the test device. The absolute bobbins consist of two windings, one receiver and the other one transmitter bobbin. In the experiments, two bobbins with a radius of 63 mm were used.

During the tests, 15 test reference components, which are kept at 860°C for an hour, cooled in oil at 70°C, then tempered at 590°C for 2 hours and cooled in the air and ensured with having required specialities, introduced to test device and their tolerance areas was created. During the introduction, impedance values of bobbins for 8 different frequencies were measured (Table 3).

The measured impedance values in the impedance plane diagram are shown in Fig. 9 for each frequency. Shown in the diagram are the tip points of UM impedance vectors which are measured by binding of compensation and test windings in opposite directions. The tolerance areas for each frequency were controlled. The impedances of the reference components have formed a good tolerance area, distributed normally. The causes of small dispersions are the dimensional tolerances, the small changes in compound, the small changes in heat treatment and the different locating of components in test bobbin. The tolerance areas built up for 8 different frequencies are particularly shown in Fig. 10.

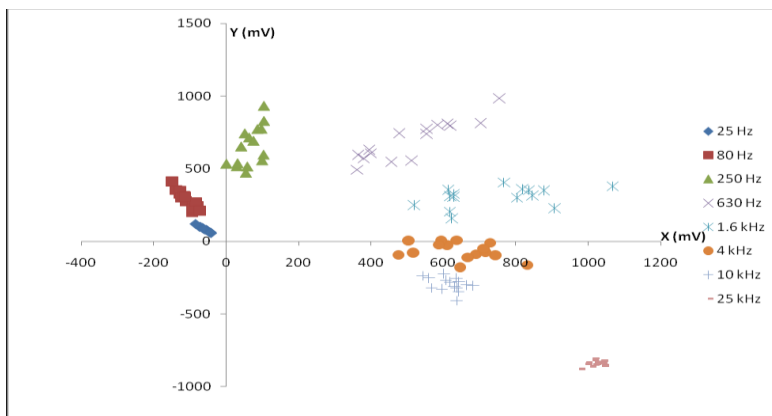


**Fig. 9** Illustration of reference components impedances in impedance plane



**Table 3**

The convenient test samples impedance values of 8 different frequencies (Hz)

No		25	80	250	630	1600	4000	10000	25000
R1	X (mV)	-51	-79	59	380	619	610	618	1022
	Y (mV)	74	244	515	572	312	-25	-280	-832
R2	X (mV)	-58	-111	42	478	767	729	682	1041
	Y (mV)	81	277	653	743	405	-10	-304	-852
R3	X (mV)	-54	-91	104	512	623	476	543	1014
	Y (mV)	79	270	597	557	157	-93	-237	-806
R4	X (mV)	-42	-94	1	395	628	594	636	1036
	Y (mV)	58	201	534	631	326	7	-254	-837
R5	X (mV)	-46	-87	30	365	614	636	643	1031
	Y (mV)	65	221	517	595	354	8	-278	-837
R6	X (mV)	-74	-139	105	703	907	646	568	996
	Y (mV)	101	353	829	815	227	-179	-320	-833
R7	X (mV)	-66	-128	87	619	846	690	630	1015
	Y (mV)	94	326	773	797	316	-89	-313	-848
R8	X (mV)	-46	-92	32	400	628	587	607	1019
	Y (mV)	63	221	537	607	308	-23	-267	-829
R9	X (mV)	-72	-127	98	611	878	744	642	1007
	Y (mV)	102	349	775	809	351	-95	-346	-859
R10	X (mV)	-62	-124	52	584	836	716	637	1019
	Y (mV)	86	303	743	802	352	-74	-319	-843
R11	X (mV)	-55	-84	100	456	618	516	560	1013
	Y (mV)	81	270	558	548	204	-78	-252	-817
R12	X (mV)	-85	-150	105	755	1068	832	637	975
	Y (mV)	121	411	933	985	379	-163	-408	-880
R13	X (mV)	-65	-116	64	553	818	711	664	1040
	Y (mV)	93	310	715	774	360	-49	-300	-855
R14	X (mV)	-43	-73	55	361	519	503	601	1038
	Y (mV)	63	211	472	492	251	4	-223	-820
R15	X (mV)	-63	-113	76	553	804	667	596	994
	Y (mV)	89	306	692	739	300	-110	-328	-844

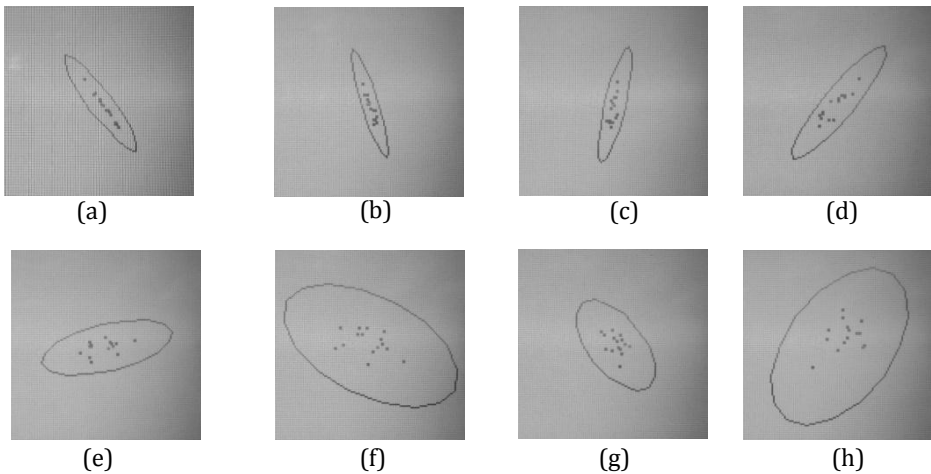


**Fig. 10** Tolerance areas for reference materials: (a) 25 Hz, (b) 80 Hz, (c) 250 Hz, (d) 630 Hz, (e) 1600 Hz, (f) 4000 Hz, (g) 10000 Hz and (h) 25000 Hz.

After formation of tolerance areas, the components obtained from faulty heat treatment processes (not appropriate) were relatively tested and their bobbin impedance values

were recorded. Firstly, test samples that are subjected to the same heat treatment process as reference components but separately charged were tested and separated successfully. Impedance values of the components are shown in the impedance plane compared with the reference components in Fig. 11.

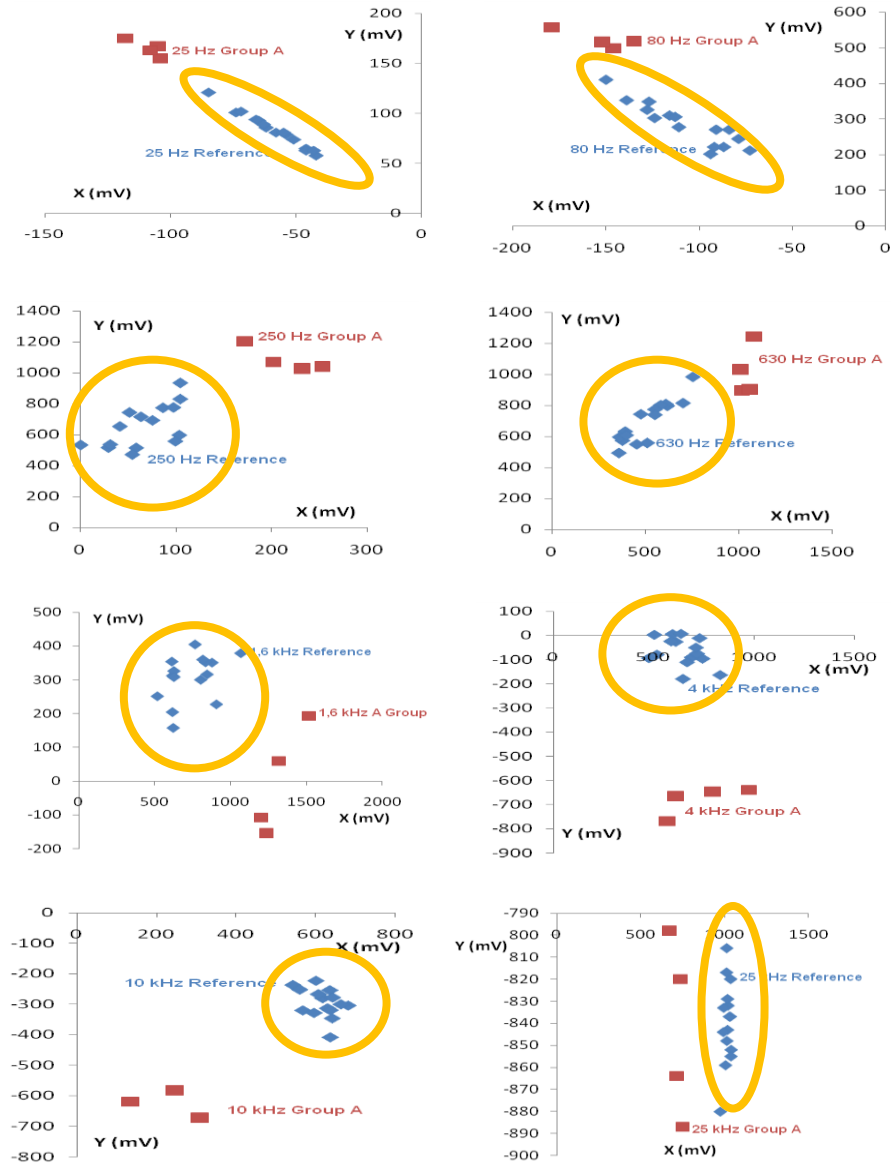


**Fig.11** Test samples of Group A is compared with reference parts on impedance plane for 25 Hz, 80 Hz, 250 Hz, 630 Hz, 1600 Hz, 4000 Hz, 10000 Hz, 25000 Hz impedances respectively

**Table 4**

Test samples impedance values of 8 different frequencies (Hz)

No		25	80	250	630	1600	4000	10000	25000
1	X (mV)	-104	-146	232	1017	1202	611	245	737
	Y (mV)	155	498	1026	896	-108	-665	-582	-820
2	X (mV)	-105	-135	253	1059	1236	568	134	671
	Y (mV)	167	518	1041	902	-154	-769	-620	-798
3	X (mV)	-118	-179	172	1081	1517	975	395	751
	Y (mV)	175	557	1203	1243	193	-640	-709	-887
4	X (mV)	-108	-152	202	1010	1318	794	309	714
	Y (mV)	163	517	1070	1033	59	-646	-672	-864

#### 4. Results

As can be seen from the tables and figures given above, as heat treatment conditions are changed, microstructures and stiffness differences that can be occurred especially on the surface and locations next to the surface of components cause some changes in permeability and particularly at high test frequencies. Since the Eddy current can outshine by causing large changes in the bobbin impedances, in case of such a test or separation, 5 kHz or upper test frequencies must be applied. In case of mixed materials, low frequencies, especially 630 Hz can be used effectively. Similar test systems will be used in cast and forging industry for structural tests of different types of components.

#### References

1. Ucmihoto T, Takagi T, Konoplyuk S, Abe T, Huang H and Kurosawa M. Eddy current evaluation of cast iron for material characterization. *Journal of Magnetism and Magnetic Materials*, 2003; 258–259, 493 – 496.
2. Konoplyuk S, Abe T, Uchimoto T, Takagi T, Huang H and Kurosawa M. Characterization of ductile cast iron by Eddy current method. *NDT&E International*, 2005; 38(8): 623 – 626.
3. Kahn SH, Ali F, Khan AN and Iqbal MA. Eddy current detection of changes in stainless steel after cold reduction. *Computational Materials Science*, 2008; 43: 623 – 628.
4. Kahn SH, Ali F, Khan AN and Iqbal MA. Pearlite determination in plain carbon steel by Eddy current method. *Journal of Processing Technology*, 2008; 300: 316 – 318.
5. Mercier D, Lesage J, Decoopman X and Chicot D. Eddy currents and hardness testing for evaluation of steel decarburizing. *NDT&E International*, 2006; 39: 652 – 660.
6. Maluba-Bafubiandi AF, Waanders FB and Jones C. Retained austenite phase in (26.5%Cr, 2.6%C) white cast iron studied by means of CEMS and Eddy current. *Hyperfine Interactions*, 2002; 139 – 140, 455 – 462.
7. Rajkumar KV, Rao BPC, Sasi B, Kumar A, Jayakumar T, Raj B and Ray KK. Characterization of aging behaviour in M250 grade maraging steel using Eddy current non-destructive methodology. *Material Science and Engineering*, 2007; 464: 233 – 240.
8. Zergoug M, Lebaili S, Boudjellal H and Benchaala A. Relation between mechanical microhardness and impedance variations in Eddy current testing. *NDT&E International*, 2004; 37: 65 – 72.